VIP Lithium Batteries Very Important Paper

International Edition: DOI: 10.1002/anie.201911724
German Edition: DOI: 10.1002/ange.201911724

A Sustainable Solid Electrolyte Interphase for High-Energy-Density Lithium Metal Batteries Under Practical Conditions

*Xue-Qiang Zhang[+], Tao Li[+], Bo-Quan Li, Rui Zhang, Peng Shi, Chong Yan, Jia-Qi Huang, and Qiang Zhang**

Abstract: *High-energy-density Li metal batteries suffer from a short lifespan under practical conditions, such as limited lithium, high loading cathode, and lean electrolytes, owing to the absence of appropriate solid electrolyte interphase (SEI). Herein, a sustainable SEI was designed rationally by combining fluorinated co-solvents with sustained-release additives for practical challenges. The intrinsic uniformity of SEI and the constant supplements of building blocks of SEI jointly afford to sustainable SEI. Specific spatial distributions and abundant heterogeneous grain boundaries of LiF, LiN_xO_y, and Li_2O effectively regulate uniformity of Li deposition. In a Li metal battery with an ultrathin Li anode (33 μm), a high-loading $LiNi_{0.5}Co_{0.2}Mn_{0.3}O_2$ cathode (4.4 mAh cm^{-2}), and lean electrolytes (6.1 g Ah^{-1}), 83% of initial capacity retains after 150 cycles. A pouch cell (3.5 Ah) demonstrated a specific energy of 340 Wh kg^{-1} for 60 cycles with lean electrolytes (2.3 g Ah^{-1}).*

Introduction

The rapidly increasing demands from portable electronics, electric vehicles, and smart grids have driven intensive researches on secondary high-energy-density batteries. Lithium (Li) metal anode provides various opportunities for high-energy-density battery systems due to its high theoretical specific capacity (3860 mAh g^{-1}) and low reduction potential (−3.04 V vs. standard hydrogen electrode).[1,2] One of the most promising practical Li metal battery systems is to couple Li metal anode with high-voltage and high-specific-capacity nickel (Ni)-rich $LiNi_xCo_yMn_{1-x-y}O_2$ (NCM) cathode.[3,4]

For practical Li metal batteries with a specific energy of more than 300 Wh kg^{-1} at cell level with Ni-rich NCM cathode, practical conditions including ultrathin Li anode (< 50 μm), high loading cathode (> 4 mAh cm^{-2}, i.e., high cycling capacity of Li per cycle), and lean electrolytes (< 3 g Ah^{-1}) are necessary.[5,6] However, mild conditions, including thick Li anode (> 200 μm), low loading cathode (< 1 mAh cm^{-2}), and flooded electrolytes (> 30 g Ah^{-1}), are currently employed, which contributes to fundamental understanding and the pioneer design of SEI on Li metal anode (Figure 1 a).[4,7] Compared with the stable SEI on graphite anode during thousands of cycles, the SEI on Li metal anode crumbles easily due to Li dendrites, which is severely aggravated under practical conditions.[8] Consequently, the gap between academical researches and practical applications in designing SEI for Li metal anode is far more challenged than graphite anode.[9] Actually, the design of SEI under mild conditions is quite difficult to meet the demands of SEI under practical conditions,[10,11] inducing extremely short lifespan of practical Li metal batteries. Therefore, the design principles of SEI on Li metal anode applied to practical conditions are highly required.

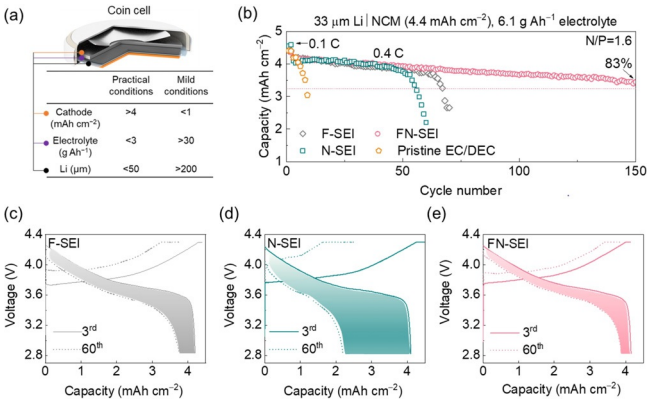

Figure 1. a) Comparison between practical conditions and mild conditions in a coin cell. b) Cycling performance of Li | NCM523 batteries with different types of SEI at 0.4 C after two formation cycles at 0.1 C. The red dashed line indicates 80% capacity retention of the initial discharge capacity at 0.4 C. c)–e) Corresponding voltage profiles of Li | NCM523 batteries after 3 and 60 cycles with c) F-SEI, d) N-SEI, and e) FN-SEI.

Generally, the formation of Li dendrites was induced by non-uniform SEI during the plating process in Li metal batteries.[12,13] The growth of Li dendrites cracks fragile SEI during Li plating, and then induces side reactions between fresh Li and electrolyte,[14] i.e., SEI precursors. Afterwards during Li stripping process, parts of the plated Li loses electronic contact with the current collectors forming dead Li

[*] X.-Q. Zhang,[+] T. Li,[+] B.-Q. Li, R. Zhang, P. Shi, Prof. Q. Zhang
Beijing Key Laboratory of Green Chemical Reaction Engineering and Technology, Department of Chemical Engineering
Tsinghua University, Beijing 100084 (P. R. China)
E-mail: zhang-qiang@mails.tsinghua.edu.cn
C. Yan, Prof. J.-Q. Huang
Advanced Research Institute of Multidisciplinary Science
Beijing Institute of Technology
Beijing 100081 (P. R. China)
[+] These authors contributed equally to this work.

Supporting information (including fabrication of the sustained-release membrane, the preparation of electrolyte, electrochemical measurements, and characterization) and the ORCID identification number(s) for the author(s) of this article can be found under: https://doi.org/10.1002/anie.201911724.

due to uneven stripping rate,[15] which also causes the depletion of fresh Li. Moreover, the depletion amount of fresh Li and electrolyte per cycle increase with the increasing cycling capacity, i.e., high loading cathode of practical conditions. Therefore, intrinsically uniform SEI is the footstone of the design principles of SEI under practical conditions to regulate Li deposition and mitigate the depletion of SEI precursors.

Adequate supplements of SEI precursors must be taken into consideration in addition to the intrinsic uniformity of SEI when comes to repeated plating/stripping processes under practical conditions. The cracks and reconstructions of SEI are hardly to avoid with large amounts of cycled Li during repeated cycles due to Li dendrites and large volume change, which depletes SEI precursors continuously. At subsequent cycles, uniform SEI formed at initial cannot maintain once any indispensable component of SEI precursors uses up, especially with limited Li and lean electrolyte in practical Li metal batteries, which leads to rapidly irreversible battery decay.[16] Therefore, a sustainable SEI, which concurrently ensures the intrinsic uniformity of SEI and the adequate supplements of building blocks of SEI, emerges as a fresh design principle of SEI for practical Li metal batteries.

Although the application of artificial films[17–20] and structured hosts[21–24] can mitigate Li dendrites growth effectively, yet the intrinsic SEI remains unchanged and becomes the bottleneck of practical Li metal batteries. Electrolyte plays a vital role in regulating the uniformity of SEI.[25–29] Tremendous efforts have been devoted to constructing intrinsically uniform SEI by regulating the electrolyte solvation, i.e., the components and structure of electrolyte, such as concentrated electrolyte,[30–34] fluorinated electrolyte,[35–37] and sacrificial additives.[38–40] Among various approaches, LiF-rich SEI (F-SEI) and LiN_xO_y-contained SEI (N-SEI) have arisen as exemplary methods to stabilize Li metal under mild conditions recently. F-SEI is generated by fluorinated solvents or Li salts[37,41–45] and N-SEI is constructed by $LiNO_3$ additives in carbonate or ether electrolyte,[40,46–51] respectively. Generally, F-SEI and N-SEI formed by additives as SEI precursors (< 5%, by weight or volume) cannot maintain sustainable due to irreversible exhaustion of limited additives under practical conditions.[52,53] In order to avoid the rapid depletion, F-SEI induced by co-solvent[45] and N-SEI formed by sustained-release method[49,54] have been put forward. Nevertheless, the sustainability of F-SEI or N-SEI under practical conditions (Figure 1a), including ultrathin Li anode (< 50 μm), high loading NCM523 cathode (> 4 mAh cm^{-2}, measured value) and lean electrolytes (< 3 g Ah^{-1}), has never been evaluated. Furthermore, sustainable SEI by combining of F-SEI and N-SEI in carbonate electrolyte remains an unexplored area in practical Li metal batteries, especially in pouch cells.

In this contribution, sustainable SEI was proposed as a fresh design principle in response to challenges from practical conditions. The sustainability of F-SEI generated by fluoroethylene carbonate (FEC) as a co-solvent and N-SEI formed by sustained-release of $LiNO_3$ was firstly investigated under practical conditions owing to the huge difference in battery performance between practical and mild conditions (Figure S1). Then, the rational combination of F-SEI and N-SEI to construct sustainable fluorinated-nitrided SEI (FN-SEI) in carbonate electrolyte was developed. In a Li metal battery composed of an ultrathin Li anode (33 μm), a high loading $LiNi_{0.5}Co_{0.2}Mn_{0.3}O_2$ (NCM523) cathode (4.4 mAh cm^{-2}), and lean electrolytes (6.1 g Ah^{-1}), FN-SEI contributed to a capacity retention of 83% after 150 cycles compared to 4 cycles by pristine SEI. Based on the analysis of components and structure of FN-SEI, LiF, LiN_xO_y, and Li_2O dominate in the components of SEI and exhibit specific spatial distributions vertically. The abundant heterogeneous grain boundaries among LiF, LiN_xO_y, and Li_2O contribute to uniform and rapid diffusion of Li ions through SEI, which guarantees uniform Li deposition. The intrinsic uniformity of SEI and the constant supplements of building blocks of SEI jointly afford to sustainable SEI under practical conditions. Consequently, the effect of sustainable FN-SEI was demonstrated in an aggressive pouch cell with specific energy of 340 Wh kg^{-1} at cell level (including all parts of a pouch cell) with lean electrolytes (2.3 g Ah^{-1}) while no external pressure was employed. Furthermore, the generality of sustainable SEI was also verified by the rational design of fluorinated-sulfurized SEI (FS-SEI) in practical Li metal batteries.

Results and Discussion

Appropriate electrolyte systems are required to evaluate the sustainability of F-SEI and N-SEI under practical conditions. Specifically, 1.0 M hexafluorophosphate ($LiPF_6$) in FEC/dimethyl carbonate (DMC) (1:4, by volume) and 1.0 M $LiPF_6$ in ethylene carbonate (EC)/diethyl carbonate (DEC) (1:1, by volume) with a $LiNO_3$ sustained-release membrane (Supporting Information, Figure S2) were chosen to obtain F-SEI and N-SEI, respectively. FEC as a co-solvent and the sustained release of $LiNO_3$ were chosen to avoid the rapid depletion of SEI precursors. The thickness of Li anode, the cathode loading, and the amount of electrolyte are the key parameters that dictate the cycling performance and specific energy of Li metal batteries. Here, practical conditions, including ultrathin Li anode (33 μm), high loading NCM523 cathode (4.4 mAh cm^{-2}) and lean electrolyte (6.1 g Ah^{-1}) were applied to evaluate the performance of SEI in practical Li metal batteries. The cycle life under practical conditions is one-eighth of that under mild conditions employed in most previous reports (Figure 1a; Supporting Information, Figure S1), including thick Li anode (> 200 μm), low loading cathode (< 1 mAh cm^{-2}), and flooded electrolytes (> 30 g Ah^{-1}). Batteries with electrolyte (< 6.1 g Ah^{-1}) cannot work normally in coin cells but work well in pouch cells because there is more useless space in coin cells to adsorb electrolyte. Therefore, the battery performance in coin cells under above practical conditions is recommended to predict the performance of electrolyte or other strategies in pouch cells to bridge the gap between academic achievements and practical applications.

Under practical conditions, Li | NCM523 batteries using common electrolyte (1.0 M $LiPF_6$ in EC/DEC, 1:1 by volume, denoted as pristine EC/DEC) failed rapidly after only 4 cycles

(Figure 1b). The benchmark of cycle life is based on the 80% capacity retention of the initial discharge capacity at 0.4C. The fresh Li has been totally depleted to form thick dead Li, which accounts for drastic capacity decay (Supporting Information, Figure S3). The thickness of dead Li is nearly 5 times of initial fresh Li. The Li | NCM523 batteries with F-SEI decayed after 64 cycles, and the Li | NCM523 batteries with N-SEI slumped after 53 cycles. Both F-SEI and N-SEI exhibited rapid increase of cell overpotentials during cycling (Figure 1c,d), indicating that the sustainability of sole F-SEI or N-SEI is limited.

Notably, the cycle life of Li | NCM523 batteries with FN-SEI was extended significantly, which demonstrates a capacity retention of 83% after 150 cycles. Moreover, the increase of overpotential within the first 60 cycles was effectively decreased (Figure 1e). Li metal anode was protected primarily so that the cycled Li anode with FN-SEI after 150 cycles also worked well when pairing with fresh NCM523 cathode (Supporting Information, Figure S4), further illustrating the sustainability of FN-SEI. Furthermore, improved rate performance was also achieved with FN-SEI. With the rate increasing from 0.1C to 2.0C, Li | NCM523 batteries with FN-SEI showed better rate performance than F-SEI and N-SEI (Supporting Information, Figure S5). The above results confirm the significant sustainability of FN-SEI in improving the lifespan of Li metal batteries.

The uniformity of SEI is the prerequisite for sustainable SEI and Li deposition morphology is the direct evidence for the uniformity of SEI.[12,55,56] Li deposition morphology after the first Li plating process was investigated by scanning electron microscopy (SEM) to gain insights into the uniformity of SEI. Remarkable differences in Li deposition morphology were observed. A Li whisker with a diameter of 2 μm was observed in pristine EC/DEC electrolyte (Supporting Information, Figure S6). In the case of F-SEI, the diameter of Li whisker was 6-fold larger than that in pristine EC/DEC electrolyte although the Li deposition remained whisker-shaped (Figure 2a). For N-SEI, Li depositions are whisker-like but the compactness is significantly inferior to that with F-SEI (Figure 2b). In the case of FN-SEI, compact deposition of large Li nodules (25 μm in diameter) were observed (Figure 2c), which is considered to greatly mitigate the parasitic reactions with electrolyte due to decreased reaction surface area and is less likely to penetrate separators. The thickness of dead Li with F-SEI was 180 μm after 100 cyles and N-SEI was 153 μm only after 45 cycles (Figure 2d,e). In comparison, a Li metal anode with a sustainable FN-SEI demonstrated a much less thickness of dead Li (133 μm) even after 200 cycles (Figure 2f). The fresh Li nearly becomes dead Li and induces large volume change when batteries fail (Supporting Information, Figure S7). Obviously, FN-SEI demonstrates the minimum volume expansion, which reconfirms that less dead Li and side reactions generate in case of FN-SEI due to much compact Li deposition. FN-SEI contributes to higher Coulombic efficiency, less dead Li formation, and higher safety compared with F-SEI and N-SEI.

The interfacial evolution of Li | NCM523 batteries with different types of SEI was further investigated by electrochemical impedance spectroscopy (EIS), where the semicircle in the high-frequency region is designated to the migration of Li ions through SEI (R_{SEI}) and the semicircle in middle-frequency region is the resistance of charge transfer (R_{ct}).[57] In general, NCM cathode is relatively stable when charged to 4.3 V. Therefore, the deterioration of Li metal anode affords the dominated interfacial impedance change in Li | NCM523 batteries. Both R_{SEI} and R_{ct} increased from the first to the 100th cycle in the following order: N-SEI > F-SEI > FN-SEI (Figure 2g,h; Supporting Information, Figure S8 and Table S1). The larger increase in R_{SEI} occurs with F-SEI and N-SEI owing to continuous side reactions on Li metal. The accompanying drastic increase in R_{ct} is from the accumulation of porous and thick dead Li, which resembles to the results in Li | Li symmetric cells (Supporting Information, Figure S9). In contrast, the increase in R_{SEI} and R_{ct} with FN-SEI is much smaller. The results of interfacial evolution further demonstrate that FN-SEI significantly decreases the interfacial resistance via enhancing the uniformity of Li depositions and suppressing the formation of dead Li.

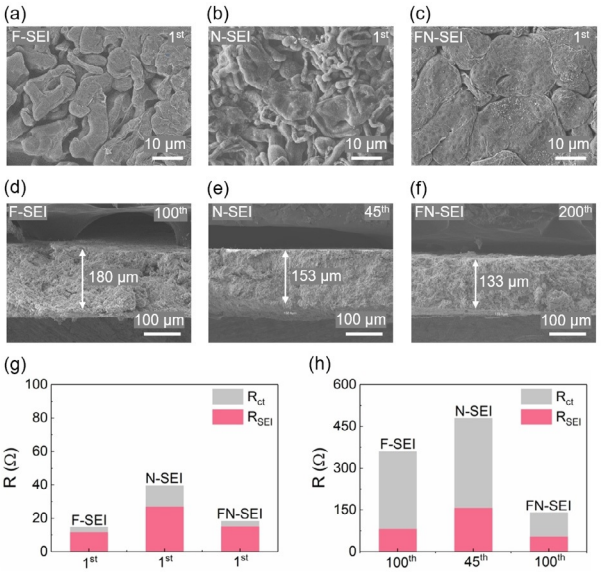

Figure 2. Li deposition morphologies in Li | NCM523 batteries with different types of SEI. a)–c) The Li deposition morphologies of a) F-SEI, b) N-SEI, and c) FN-SEI after the first deposition process. The deposition was carried out at a current density of 0.15 mA cm^{-2} with a capacity of 2.5 mAh cm^{-2} in Li | NCM523 batteries. d)–f) Cross-sectional views of cycled Li metal anode retrieved from Li | NCM523 batteries with d) F-SEI, e) N-SEI, and f) FN-SEI after 100, 45, and 200 cycles, respectively. g),h) The evolutions of interfacial resistance of Li | NCM523 batteries with different types of SEI after g) 1 and h) 100 cycles (45 cycles for N-SEI).

X-ray photoelectron spectroscopy (XPS) analysis was carried out on the cycled Li metal to further disclose the features of SEI. The organic layer exists on the top surface of SEI (Supporting Information, Figures S10–S12). The types and spatial distribution of inorganics vary with the types of SEI beneath the organic layer. In F-SEI, LiF distributes uniformly at different depths (Figure 3a,d), which is mainly from the decomposition of FEC as reported.[45,52] LiF has been known to increase the uniformity of Li deposition.[35,58]

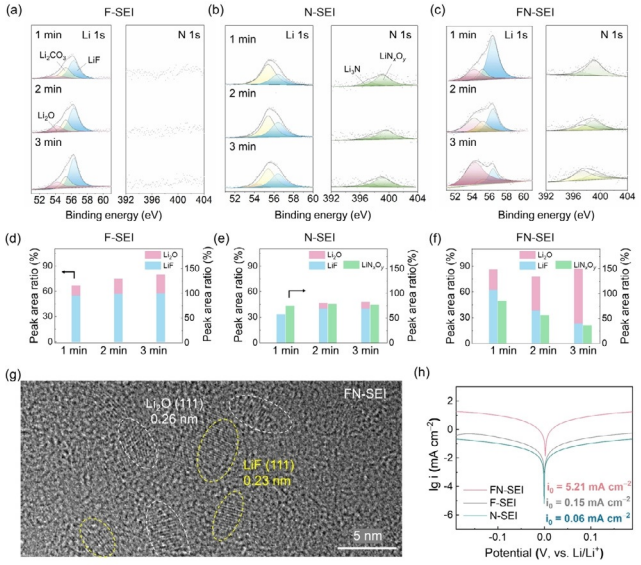

Figure 3. a)–c) XPS spectra depth profiles of a) F-SEI, b) N-SEI, and c) FN-SEI on Li metal anode after etching. d)–f) The peak area ratio of LiF, LiN_xO_y, and Li_2O in d) F-SEI, e) N-SEI, and f) FN-SEI. g) High-resolution TEM image of the FN-SEI on Li metal retrieved from Li | NCM523 batteries after one formation cycles. h) Tafel plots obtained from a cyclic voltammetry test in Li | Li cells with a scan rate of 1.0 $mV s^{-1}$.

In N-SEI, the content of LiF significantly reduces according to the atomic concentration of F (Supporting Information, Figure S13) because the formation of LiF only depends on the decomposition of $LiPF_6$. The emerge of LiN_xO_y indicates that $LiNO_3$ engages in the formation of SEI, and thus sustained-release of $LiNO_3$ is effective in SEI modification (Figure 3b).[54] LiN_xO_y also has a positive effect on improving the ion transport property of SEI.[40,53] The content of LiF and LiN_xO_y demonstrates negligible changes with depth in F-SEI and N-SEI, respectively. In contrast, the spatial distribution of inorganics in FN-SEI varies greatly with depth (Figure 3c,f). The content of LiF decreases with increasing depth although the relative amount of LiF is very high. In contrast, the content of Li_2O increases with the rise of depth in FN-SEI. Compared with F-SEI, it is inferred that $LiNO_3$ additives greatly alters the components and the spatial distribution of inorganics in F-SEI to form FN-SEI. Moreover, the introduction of $LiNO_3$ promotes the generation of much Li_2O in the closest vicinity of Li metal in the formation processes of FN-SEI. LiF, LiN_xO_y, and Li_2O dominate in the components of SEI and display specific spatial distributions in SEI, which improve the intrinsic uniformity and ion transport capability of SEI significantly.

FN-SEI was further detected via transmission electron microscopy (TEM) equipped with double spherical aberration correctors (Figure 3g), in which different crystalline inorganics (ca. 5 nm in diameter), mainly LiF and Li_2O, can be identified evidently. No N-containing crystalline inorganic compound was observed but N element can be detected via the energy dispersion spectrum elemental mappings (Supporting Information, Figure S14). LiF, LiN_xO_y, and Li_2O are mixed in spatial, forming abundant heterogeneous grain boundaries. The grain boundaries between inorganics significantly impact the diffusion of Li ions in SEI.[15,55] There are much different grain boundaries in SEI, mainly including heterogeneous and homogeneous grain boundaries. The heterogeneous grain boundaries are proven to exhibit the faster diffusion of Li ions than the homogeneous grain boundaries.[59] The diffusion of Li ions in SEI are positively correlated with exchange current density (I_0, Figure 3h).[60,61] The exchange current density of FN-SEI ($I_0 = 5.21\ mA\,cm^{-2}$) is much larger than that in F-SEI ($I_0 = 0.15\ mA\,cm^{-2}$) and N-SEI ($I_0 = 0.06\ mA\,cm^{-2}$). Compared with F-SEI and N-SEI, more abundant heterogeneous grain boundaries among LiF, LiN_xO_y, and Li_2O in FN-SEI in the closest vicinity of Li metal contribute to rapid Li ions transport definitively. Furthermore, the abundant heterogeneous grain boundaries also benefit uniform Li ions diffusion, which have been proved by uniform Li deposition.

Sustainable FN-SEI was further employed in a practical Li | NCM523 pouch cell of 3.5 Ah with a specific energy of 340 $Wh\,kg^{-1}$ at cell level with lean electrolytes (2.3 $g\,Ah^{-1}$) to evaluate the potential of the fresh design principle. The mass of all parts of the pouch cell is included into the calculation of the specific energy (for detailed pouch cell parameters see the Supporting Information, Figure S15 and Table S2). The Li | NCM523 pouch cell with the specific energy of 340 $Wh\,kg^{-1}$ at cell level was achieved and more than 60 stable cycles with a capacity retention of 90% were demonstrated without no external pressure (Figure 4c,d). The stable cycle for Li metal pouch cells is more challenged without external pressure than that with external pressure. The pouch cell was disassembled after 45 cycles to investigate the protection effect of FN-SEI on Li metal anode and analyze the decay mechanism of pouch cells. The cycled Li surface with sustainable FN-SEI maintained smooth and showed good metallic luster (Supporting Information, Figures S16, S17a,b), while Li anode without FN-SEI exhibited highly porous and pulverized morphology

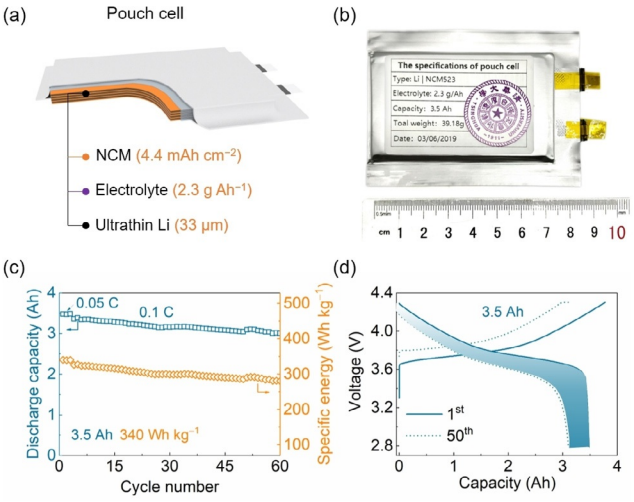

Figure 4. a) A pouch cell under practical conditions with ultrathin Li anode, lean electrolytes, and high-loading cathode. b) Digital image of a pouch cell with specific energy of 340 $Wh\,kg^{-1}$ at cell level and c) the corresponding cycling performance at 0.1 C after three formation cycles at 0.05 C. d) The voltage profiles of pouch cells at 1st and 50th cycle.

(Supporting Information, Figures S16, S17c,d). Base on the thickness estimation of remaining fresh Li (48 μm; Supporting Information, Figure S17b), only 27% of the pristine Li (66 μm, double sides Li on current collector in pouch cells) was consumed after 45 cycles with FN-SEI protection, proving that sustainable FN-SEI suppresses the depletion of fresh Li effectively. Sustainable FN-SEI significantly protects Li metal and contributes to stable cycles of Li metal pouch cells, which makes much sense for practical applications.

To further confirm the generality of design principle of SEI in this work, another example, Li_2SO_4, was rationally designed based on the above insights and understanding to construct sustainable FS-SEI. The cycle life of Li | NCM523 batteries with FS-SEI was extended significantly when compared with F-SEI (Supporting Information, Figure S18a). The increase of overpotential within the first 60 cycles was also effectively decreased (Supporting Information, Figure S18b,c), which confirms the effectiveness of sustainable SEI in Li metal batteries under harsh conditions. The components and the corresponding distribution in FS-SEI resemble to the features of FN-SEI (Supporting Information, Figure S19). There is much LiF and Li_2O in FS-SEI, in which Li_2O increases and LiF decreases with the increasing depth. Moreover, there are lithium sulfates ($LiSO_x$), which is due to the decomposition of Li_2SO_4. The above analyses demonstrate the vital role of components and their distributions in regulating Li ion diffusion and deposition. The successful extension of FS-SEI confirms the generality of design principles of sustainable SEI and the fundamental understanding of SEI under practical applications.

Conclusion

Sustainable SEI under harsh conditions, including ultrathin Li anode (< 50 μm), high loading cathode (> 4 mAh cm^{-2}), and lean electrolytes (< 3 g Ah^{-1}), was proposed to promote the development of practical Li metal batteries in this work. A rational electrolyte strategy was developed to construct sustainable SEI, in which the intrinsic uniformity of SEI and the constant supplements of building blocks of SEI jointly afford to sustainable SEI. LiF, LiN_xO_y, and Li_2O display specific vertically spatial distribution and the abundant heterogeneous grain boundaries in FN-SEI contribute to uniform and rapid Li-ion transport. Much improved uniformity of SEI effectively regulates uniformity of Li deposition and decreases the depletion of SEI precursors per cycle, which is the foundation of sustainable SEI. In a practical Li metal battery, FN-SEI contributed to a capacity retention of 83% after 150 cycles compared to 4 cycles by pristine SEI, 64 cycles by F-SEI, and 53 cycles by N-SEI, respectively. More importantly, a practical pouch cell with specific energy of 340 Wh kg^{-1} at cell level maintained more than 60 cycles with 90% capacity retention without no external pressure. Furthermore, the generality of sustainable SEI was also verified by the rational design of FS-SEI in practical Li metal batteries. This work develops fresh design principles of SEI for high-energy-density Li metal batteries and other types of batteries, especially under practical conditions.

Acknowledgements

This work was supported by National Key Research and Development Program (2016YFA0202500 and 2015CB932500), National Natural Science Foundation of China (21676160, 21825501, 21805161, and U1801257), and the Tsinghua University Initiative Scientific Research Program.

Conflict of interest

The authors declare no conflict of interest.

Keywords: electrolytes · lithium batteries · pouch cells · solid electrolyte interphases

How to cite: *Angew. Chem. Int. Ed.* **2020**, *59*, 3252–3257
Angew. Chem. **2020**, *132*, 3278–3283

[1] X. B. Cheng, R. Zhang, C. Z. Zhao, Q. Zhang, *Chem. Rev.* **2017**, *117*, 10403.
[2] D. Lin, Y. Liu, Y. Cui, *Nat. Nanotechnol.* **2017**, *12*, 194.
[3] S. Chen, C. Niu, H. Lee, Q. Li, L. Yu, W. Xu, J.-G. Zhang, E. J. Dufek, M. S. Whittingham, S. Meng, J. Xiao, J. Liu, *Joule* **2019**, *3*, 1094.
[4] J. Liu, Z. N. Bao, Y. Cui, E. J. Dufek, J. B. Goodenough, P. Khalifah, Q. Y. Li, B. Y. Liaw, P. Liu, A. Manthiram, Y. S. Meng, V. R. Subramanian, M. F. Toney, V. V. Viswanathan, M. S. Whittingham, J. Xiao, W. Xu, J. H. Yang, X. Q. Yang, J. G. Zhang, *Nat. Energy* **2019**, *4*, 180.
[5] P. Albertus, S. Babinec, S. Litzelman, A. Newman, *Nat. Energy* **2017**, *3*, 16.
[6] X. Zeng, M. Li, D. Abd El-Hady, W. Alshitari, A. S. Al-Bogami, J. Lu, K. Amine, *Adv. Energy Mater.* **2019**, *9*, 1900161.
[7] C. Niu, H. Lee, S. Chen, Q. Li, J. Du, W. Xu, J.-G. Zhang, M. S. Whittingham, J. Xiao, J. Liu, *Nat. Energy* **2019**, *4*, 551.
[8] W. Xu, J. L. Wang, F. Ding, X. L. Chen, E. Nasybutin, Y. H. Zhang, J. G. Zhang, *Energy Environ. Sci.* **2014**, *7*, 513.
[9] Y. Cao, M. Li, J. Lu, J. Liu, K. Amine, *Nat. Nanotechnol.* **2019**, *14*, 200.
[10] Z. Lin, T. Liu, X. Ai, C. Liang, *Nat. Commun.* **2018**, *9*, 5262.
[11] S. C. Nagpure, T. R. Tanim, E. J. Dufek, V. V. Viswanathan, A. J. Crawford, S. M. Wood, J. Xiao, C. C. Dickerson, B. Liaw, *J. Power Sources* **2018**, *407*, 53.
[12] M. D. Tikekar, S. Choudhury, Z. Y. Tu, L. A. Archer, *Nat. Energy* **2016**, *1*, 1.
[13] J. Betz, J. P. Brinkmann, R. Nolle, C. Lurenbaum, M. Kolek, M. C. Stan, M. Winter, T. Placke, *Adv. Energy Mater.* **2019**, *9*, 1900574.
[14] D. Aurbach, E. Zinigrad, Y. Cohen, H. Teller, *Solid State Ionics* **2002**, *148*, 405.
[15] Y. Li, W. Huang, Y. Li, A. Pei, D. T. Boyle, Y. Cui, *Joule* **2018**, *2*, 2167.
[16] S. S. Zhang, *J. Power Sources* **2006**, *162*, 1379.
[17] M. S. Kim, J.-H. Ryu, L. Y. R. Deepika, I. W. Nah, K.-R. Lee, L. A. Archer, W. Il Cho, *Nat. Energy* **2018**, *3*, 889.

[18] N. W. Li, Y. Shi, Y. X. Yin, X. X. Zeng, J. Y. Li, C. J. Li, L. J. Wan, R. Wen, Y. G. Guo, *Angew. Chem. Int. Ed.* **2018**, *57*, 1505; *Angew. Chem.* **2018**, *130*, 1521.
[19] Q. Pang, X. Liang, A. Shyamsunder, L. F. Nazar, *Joule* **2017**, *1*, 871.
[20] G. Li, Y. Gao, X. He, Q. Huang, S. Chen, S. H. Kim, D. Wang, *Nat. Commun.* **2017**, *8*, 850.
[21] C. P. Yang, Y. X. Yin, S. F. Zhang, N. W. Li, Y. G. Guo, *Nat. Commun.* **2015**, *6*, 8058.
[22] Y. Liu, D. Lin, Z. Liang, J. Zhao, K. Yan, Y. Cui, *Nat. Commun.* **2016**, *7*, 10992.
[23] C. Yang, Y. Yao, S. He, H. Xie, E. Hitz, L. Hu, *Adv. Mater.* **2017**, *29*, 1702714.
[24] S. H. Wang, J. Yue, W. Dong, T. T. Zuo, J. Y. Li, X. Liu, X. D. Zhang, L. Liu, J. L. Shi, Y. X. Yin, Y. G. Guo, *Nat. Commun.* **2019**, *10*, 4930.
[25] X. Q. Zhang, X. B. Cheng, Q. Zhang, *Adv. Mater. Interfaces* **2018**, *5*, 1701097.
[26] K. Xu, *Chem. Rev.* **2014**, *114*, 11503.
[27] D. Aurbach, Y. Talyosef, B. Markovsky, E. Markevich, E. Zinigrad, L. Asraf, J. S. Gnanaraj, H. J. Kim, *Electrochim. Acta* **2004**, *50*, 247.
[28] P. Verma, P. Maire, P. Novák, *Electrochim. Acta* **2010**, *55*, 6332.
[29] J. Wang, Y. Yamada, K. Sodeyama, C. H. Chiang, Y. Tateyama, A. Yamada, *Nat. Commun.* **2016**, *7*, 12032.
[30] S. Chen, J. Zheng, D. Mei, K. S. Han, M. H. Engelhard, W. Zhao, W. Xu, J. Liu, J.-G. Zhang, *Adv. Mater.* **2018**, *30*, 1706102.
[31] L. Suo, O. Borodin, T. Gao, M. Olguin, J. Ho, X. Fan, C. Luo, C. Wang, K. Xu, *Science* **2015**, *350*, 938.
[32] J. Qian, W. A. Henderson, W. Xu, P. Bhattacharya, M. Engelhard, O. Borodin, J. G. Zhang, *Nat. Commun.* **2015**, *6*, 6362.
[33] K. Ueno, J.-W. Park, A. Yamazaki, T. Mandai, N. Tachikawa, K. Dokko, M. Watanabe, *J. Phys. Chem. C* **2013**, *117*, 20509.
[34] J. Zheng, J. A. Lochala, A. Kwok, Z. D. Deng, J. Xiao, *Adv. Sci.* **2017**, *4*, 1700032.
[35] X. Fan, L. Chen, O. Borodin, X. Ji, J. Chen, S. Hou, T. Deng, J. Zheng, C. Yang, S.-C. Liou, K. Amine, K. Xu, C. Wang, *Nat. Nanotechnol.* **2018**, *13*, 715.
[36] X. Q. Zhang, X. Chen, X. B. Cheng, B. Q. Li, X. Shen, C. Yan, J. Q. Huang, Q. Zhang, *Angew. Chem. Int. Ed.* **2018**, *57*, 5301; *Angew. Chem.* **2018**, *130*, 5399.
[37] S. J. Park, J. Y. Hwang, C. S. Yoon, H. G. Jung, Y. K. Sun, *ACS Appl. Mater. Interfaces* **2018**, *10*, 17985.
[38] C. Z. Zhao, X. B. Cheng, R. Zhang, H. J. Peng, J. Q. Huang, R. Ran, Z. H. Huang, F. Wei, Q. Zhang, *Energy Storage Mater.* **2016**, *3*, 77.
[39] J. Qian, W. Xu, P. Bhattacharya, M. Engelhard, W. A. Henderson, Y. Zhang, J.-G. Zhang, *Nano Energy* **2015**, *15*, 135.
[40] C. Yan, Y. X. Yao, X. Chen, X. B. Cheng, X. Q. Zhang, J. Q. Huang, Q. Zhang, *Angew. Chem. Int. Ed.* **2018**, *57*, 14055; *Angew. Chem.* **2018**, *130*, 14251.
[41] J. H. Song, J. T. Yeon, J. Y. Jang, J. G. Han, S. M. Lee, N. S. Choi, *J. Electrochem. Soc.* **2013**, *160*, A873.
[42] J. Heine, P. Hilbig, X. Qi, P. Niehoff, M. Winter, P. Bieker, *J. Electrochem. Soc.* **2015**, *162*, A1094.
[43] Q. C. Liu, J. J. Xu, S. Yuan, Z. W. Chang, D. Xu, Y. B. Yin, L. Li, H. X. Zhong, Y. S. Jiang, J. M. Yan, *Adv. Mater.* **2015**, *27*, 5241.
[44] L. Suo, W. Xue, M. Gobet, S. G. Greenbaum, C. Wang, Y. Chen, W. Yang, Y. Li, J. Li, *Proc. Natl. Acad. Sci. USA* **2018**, *115*, 1156.
[45] E. Markevich, G. Salitra, F. Chesneau, M. Schmidt, D. Aurbach, *ACS Energy Lett.* **2017**, *2*, 1321.
[46] D. Aurbach, E. Pollak, R. Elazari, G. Salitra, C. S. Kelley, J. Affinito, *J. Electrochem. Soc.* **2009**, *156*, A694.
[47] S. S. Zhang, *Electrochim. Acta* **2012**, *70*, 344.
[48] S. Xiong, K. Xie, Y. Diao, X. Hong, *Electrochim. Acta* **2012**, *83*, 78.
[49] Q. Shi, Y. Zhong, M. Wu, H. Wang, H. Wang, *Proc. Natl. Acad. Sci. USA* **2018**, *115*, 5676.
[50] A. Jozwiuk, B. B. Berkes, T. Weiß, H. Sommer, J. Janek, T. Brezesinski, *Energy Environ. Sci.* **2016**, *9*, 2603.
[51] B. D. Adams, E. V. Carino, J. G. Connell, K. S. Han, R. G. Cao, J. Z. Chen, J. M. Zheng, Q. Y. Li, K. T. Mueller, W. A. Henderson, J. G. Zhang, *Nano Energy* **2017**, *40*, 607.
[52] X. Q. Zhang, X. B. Cheng, X. Chen, C. Yan, Q. Zhang, *Adv. Funct. Mater.* **2017**, *27*, 1605989.
[53] W. Li, H. Yao, K. Yan, G. Zheng, Z. Liang, Y.-M. Chiang, Y. Cui, *Nat. Commun.* **2015**, *6*, 7436.
[54] Y. Liu, D. Lin, Y. Li, G. Chen, A. Pei, O. Nix, Y. Li, Y. Cui, *Nat. Commun.* **2018**, *9*, 3656.
[55] Y. Li, Y. Li, A. Pei, K. Yan, Y. Sun, C. L. Wu, L. M. Joubert, R. Chin, A. L. Koh, Y. Yu, J. Perrino, B. Butz, S. Chu, Y. Cui, *Science* **2017**, *358*, 506.
[56] F. Shi, A. Pei, A. Vailionis, J. Xie, B. Liu, J. Zhao, Y. Gong, Y. Cui, *Proc. Natl. Acad. Sci. USA* **2017**, *114*, 12138.
[57] H. Xiang, P. Shi, P. Bhattacharya, X. Chen, D. Mei, M. E. Bowden, J. Zheng, J.-G. Zhang, W. Xu, *J. Power Sources* **2016**, *318*, 170.
[58] Y. Lu, Z. Tu, L. A. Archer, *Nat. Mater.* **2014**, *13*, 961.
[59] A. Ramasubramanian, V. Yurkiv, T. Foroozan, M. Ragone, R. Shahbazian-Yassar, F. Mashayek, *J. Phys. Chem. C* **2019**, *123*, 10237.
[60] P. Biswal, S. Stalin, A. Kludze, S. Choudhury, L. A. Archer, *Nano Lett.* **2019**, *19*, 8191.
[61] Y. He, X. Ren, Y. Xu, M. H. Engelhard, X. Li, J. Xiao, J. Liu, J. G. Zhang, W. Xu, C. Wang, *Nat. Nanotechnol.* **2019**, *14*, 1042.

Manuscript received: September 12, 2019
Accepted manuscript online: November 22, 2019
Version of record online: January 3, 2020

